GEOSCIENCES
journal homepage: www.gsjournal.ir

Mineralogy and geochemistry of Nodoushan Zn-Pb deposit: A transitional deposit in UDMA, Central Iran

Kamran Motevali[1], Mehrdad Behzadi[2*] and Mohammad Yazdi[3]

[1]*Ph.D. Student, Department of Geology, Faculty of Earth Science, Shahid Beheshti University, Tehran, Iran*
[2]*Assistant Professor, Department of Geology, Faculty of Earth Science, Shahid Beheshti University, Tehran, Iran*
[3]*Professor, Department of Geology, Faculty of Earth Science, Shahid Beheshti University, Tehran, Iran*

ARTICLE INFO

Received: 2017 November 25
Accepted: 2018 February 17
Available online: 2018 March 17

Keywords:
Vein-type
Epithermal
Zn-Pb deposit
Nodoushan

**Corresponding author:*
M. Behzadi
E-mail: m-behzadi@sbu.ac.ir

ABSTRACT

Eocene magmatism with intermediate-acid tuffs and volcanic rocks, the host to the Nodoushan deposit in Yazd province, intruded by Oligocene early diorite and later granite plutonic rocks. The former involved in iron skarn (containing epidote and euhedral grossularite) to the north and northern part of the deposit, the latter contributed to fault-controlled Zn-Pb deposit. The structural features controlled both the mineralization and consequent alterations which ranged from silicification (central) to argillic alteration (northern). Propylitic alteration and dolomitization considered the minor ones, the iron contamination of which could be provided by earlier iron mineralization. Sulfide minerals are dominantly pyrite, sphalerite and galena followed by chalcopyrite and late stage copper minerals such as covellite, digenite, bornite, chalcocite. Oxide minerals developed to the depth of 40 m as a result of faults. Sphalerite which is of high-Fe type was characterized by extensive chalcopyrite disease, the iron content of which provided by earlier iron concentration. The concentration of chalcopyrite exsolution along sphalerite margins as well as galena veinlets is due to the thermal shock of later stage hydrothermal fluids that deposited galena and chalcopyrite. Negligible fossil replacements indicate both mineralization and alteration. It was concluded that the Zn-dominant mineralization was deposited under the structural controlling faults which reflects part of its earlier iron mineralization.

1- Introduction

Urumieh-Dokhtar Magmatic Arc (UDMA) resulted from Neo-Tethys Oceanic crust subduction beneath Central Iran Micro-continent (CIM) (Shahabpour, 2007) which is important from metallogenic point of view from the very rifting to its closure (Giese, 1984). Such magmato-tectonic board is engraved by various metallogenic events that make the backbone of the old and present mining industry. This is evidenced by 2015 Iran base metals production including 1.2% copper, 0.8% lead and 1.1% zinc of the total world market production (Brown et al., 2017) as well as several archaeo-mining activities in central and southeastern Iran (Hakemi, 1997, Hauptmann, 2003; Momenzadeh, 2005) among which 4th millennium Arisman and Tepe Sialk near Kashan in UDMA (Schreiner, 2002) can be numerated.

Iran higher benefits from its favorable geological settings and associated mineralization in Iranian section of Alpine-Himalayan orogenic belt lies in its bifurcation in northwestern Iran into NW-SE trending UDMA as a result of Neo-Tethys subduction and E-W branch along northern border which resulted from Paleo-Tethys subduction.

UDMA magmatism is composed of subduction-related calc-alkaline and tholeiitic rocks based on geochemical data (Ahmad, 1993) terminated with minor shoshonitic and alkaline rocks (Omrani et al., 2008). The mineraliferous UDMA accounts for more than 20% of the total known mineralization in Iran (Najafi et al., 2012) which has been devouring voluminous exploration budgets for several decades. Steeper slope of subduction (Berberian and Berberian, 1981)

at its southern parts led to Dehaj-Sarduyieh copper district hosting well-known Sarcheshmeh porphyry Cu (-Mo) mine and other porphyry or non-porphyry copper deposit. The copper tendency in mineralization turns northwestward into lead and zinc, iron, barite, silica, perlite and finally copper and gold based on the mineral distribution map of Iran (Lotfi et al., 1993; Najafi et al., 2012) that indicates changes in mineralization mechanism along the arc (Fig.1).

The plutonic bodies in the area intruded a wide variety of geologic units where the emanating hydrothermal fluids led to various mineralization in Triassic shale and limestone [Khut Cu-Skarn (Bazin and Hubner, 1968; Yazdi, 1992), Chah Khattab Cu veins (Bazin and Hübner, 1969)], Eocene volcanic rocks [(Nodoushan Zn-Pb deposit (Taghizadeh Khajooee and Sheykhi Karizaki, 1998), Aliabad and Darreh-zereshk porphyry copper (Taghipour and Makizadeh, 2011), Surk Fe skarn mine (Minook Consulting Engineers, 1993; Makizadeh et al., 2007), Nodoushan Fe Skarn deposits (Barati, 2017) and Hourak gold mineralization)].

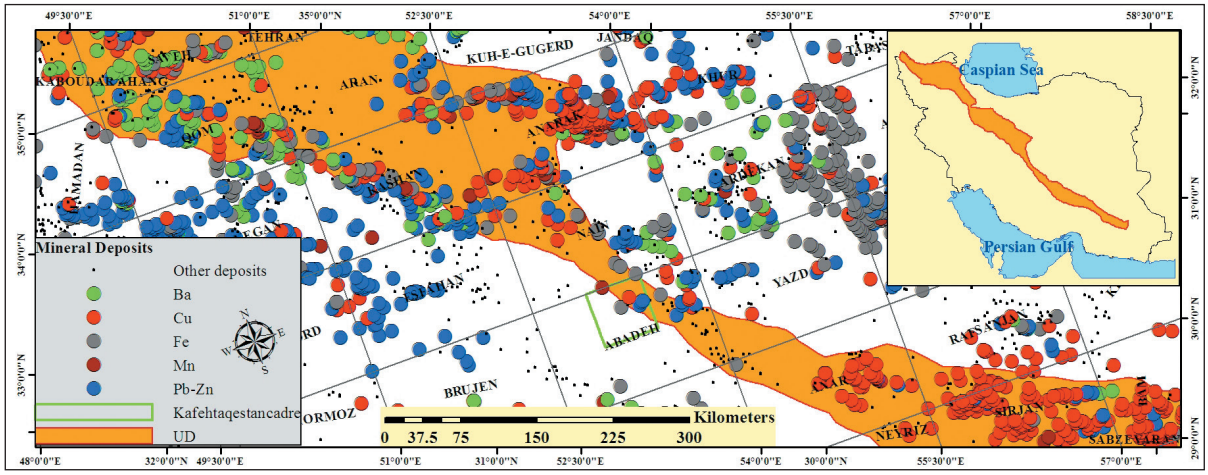

Fig. 1- A general view of UDMA (in orange) in Iran (side map) and middle UDMA mineralization (main map) bordering Sanandaj-Sirjan zone to the west and CIM to the east. The Red, blue, black, gray, brown and green circles demonstrate Cu, Zn-Pb, Fe, Mn and Ba mineralization, respectively. Small black dots are all other mineralization and Rectangles are 1:250000 geological quadrangle names. The Kafetaghestan 1:100000 map frame is demonstrated in green within Abadeh 1:250000 geological quadrangle.

The Nodoushan Zn-Pb deposit is located 120 Km west of Yazd capital city, in the Central UDMA bordering Sanandaj-Sirjan Zone (SSZ). It occurred in the transitional mineralization from copper into zinc-lead. The study on such transitional deposits and comparison of them to each other may shed light on the exploration for similar deposits. Old mining potential was evidenced by an old cave at silicified units as well as some slags five kilometers to the east of the deposit.

2- Methodology

Several field visits were made to the study area in order to delineate structural phenomena (Pre-determined by satellite images), determine geological and mineralization processes involved in the development of Zn-Pb Nodoushan deposit. Thereafter, many microscopic sections (171 thin sections and 144 polished sections) were studied over and over under the microscope to decipher more mineralization processes. These macroscopic and microscopic observations on surface and subsurface materials associated with ICP results of more than 234 samples that provided us with the evidences to determine the genesis of the deposit.

3- Geology and petrography

The oldest lithological unit cropped out in the study area is the Permian carbonate to the east of the deposit adjacent to the fault. Younger lithologies are Jurassic and Cretaceous sandstone, the latter cropped out to the west of the deposit. After such sedimentary set of deposits which ended in Cretaceous-Paleocene conglomerates, vast Eocene intermediate-acid volcanic rocks and tuffs (Fig. 2- a, b, c and e) which is the host rock to the mineralization developed in the area, locally interbedded with nummulitic limestone. The andesitic, dacitic and rhyodacitic rocks demonstrated a wide range of glass, crystal and clasts ratios to develop porphyry, lithic crystal, vitric crystal and lapilli tuffs, associated with

sporadic opaque minerals (Fig. 2- d). Sometimes lava interfingering was associated with the volcanic rocks. These rocks were intruded by acid to intermediate dikes and intrusive bodies which are younger in age than the Eocene volcanic units (Fig. 2- a and b). Earlier studies on the intrusive bodies distinguished four types of intrusions with older diorites, followed by leucogranites, granites and granodiorites, the first two were observed at the deposit district (Yajam, 2005) which was later confirmed by their U-Pb ages from their zircons to decipher earlier diorites of 30.52±0.11 Ma and later granites of 30.06±0.11 Ma (Shahsavari Alavijeh et al., 2017). The intrusions are metaluminous and are enriched in Ca, Na and Sr content. Petrochemical studies on XRF results indicated that the granitoid bodies exposed in the area, were I-type (Yajam, 2005). These bodies caused contact metamorphism, alteration and consequent mineralization. The contact metamorphism which developed limited skarn is characterized by euhedral garnet (grossularite) (Fig. 2- g).

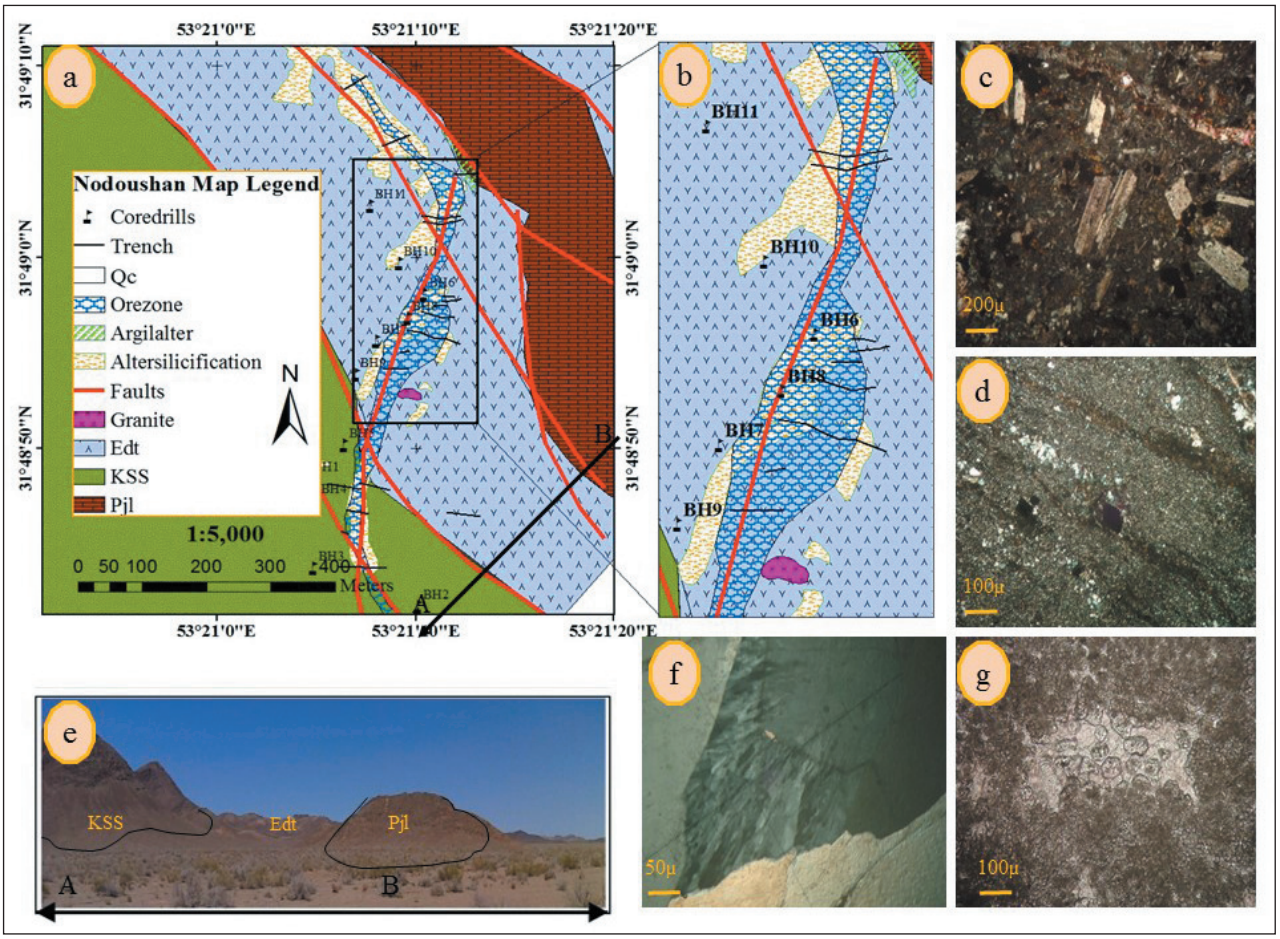

Fig. 2- The Geology of the study area a) on 1:5000 simplified map with drillpoints in black, Pjl: Permian dolomite and dolomitic limestone (Jamal formation), Kss: Cretaceous sandstone, Edt: Eocene tuffs and volcanics b) zoomed view at the deposit c) crystal vitric tuff with sporadic (×5XPL) with euhedral to subhedral opaque minerals d) lapilli tuff with euhedral opaque minerals (probably pyrite) which may indicate disseminated mineralization before main stage epithermal mineralization (×10XPL) e) A view of the study area demonstrated as AB black line on Fig. a f) graining quartz at the margin as a result of stress (×20XPL) g) skarn sample with euhedral grossularite (×10X).

Further petrochemical investigation on Tertiary dacite, andesite, olivine basalt, and also pyroclastic (crystalline tuff), and micro-granodioritic intrusive rocks indicated magmatic arc tectonic setting based on Y-Nb versus Y-Zr and Zr/Al2O3 versus TiO2/Al2O3 for the samples taken from 8 Km to the northeast of the study area. In the spider diagram normalized to MORB, HFS elements demonstrated depletion, known to be characteristic of magmatism at the volcanic arc setting. The K, Rb and Th enrichment (Etemadi et al., 2012) as well as the negative anomaly of Ti, Ta, Nb and P suggested that the rocks formed within subduction zone (Qalamqash and Mohammadiha, 2005).

The major fault in the area is Dehshir Fault trending NW-SE extending 350 Km (Berberian and King, 1981),

passing 17 Km away from northeast of the study area where it is associated with sporadic ultramafic outcrops. The performance of its dextral strike-slip fault and subsequent parallel faults led to development of a shear zone in the area. The rock assemblage at the study area is mainly associated with abundant faulting and trans-tensional ruptures (Qalamqash and Mohammadiha, 2005). These faults splitted off southward the southern margin of the volcanic rock assemblages. The offset of this generally NW-SE trending ruptured body varies up to 8 Km, more or less is intruded by plutonic bodies (diorite and granite). The offset also influenced the earlier veins up to several kilometers, an example of which was observed at Qoltuk Hill, some 2 Km southwest of the Nodoushan where it is believed to be the southern extension of the mineralized vein of Nodoushan (Taghizadeh Khajooee and Sheykhi Karizaki, 1998). The stresses on the quartz is well represented as subgrainng under the microscope (Fig. 2- f). such fracturing and faulting paved the way for structurally controlled alteration in the area (Fig. 2- a and b and 3).

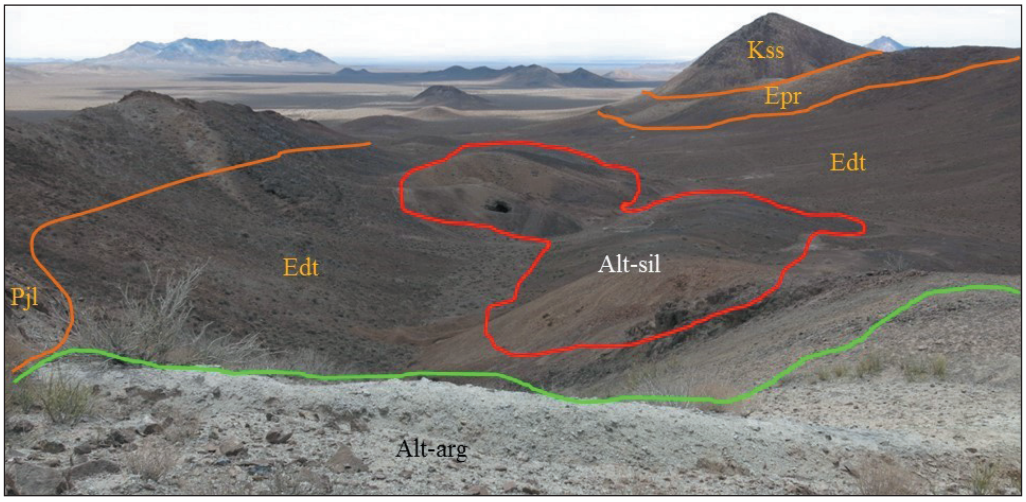

Fig. 3- A view of the study area looking southeast. Geological units are as following Pjl: Permian limestone, Edt: Eocene tuff, Epr: Eocene pyroclastics as well as Alt-sil: silicification, Alt-arg: argillic alteration.

4- Mineralization

The mineralization is hosted by Eocene rhyodacitic-dacitic to andesitic pyroclastic vitric to crystal vitric tuff and volcanic rocks intersected by veins and associated with silicification. This unit which was likely ruptured off the major volcanic assemblages to the northeast intruded by diorite and later granite intrusions of Early Miocene. The earlier diorite intrusion developed iron mineralization as skarn iron deposit to the north (Barati, 2017), characterized by skarn minerals such as euhedral (to subhedral) grossular garnet in the surrounding rocks at the northern parts of the Zn-Pb deposit but no Zn-Pb concentration determined to the north associated with iron concentration. At the northern Zn-Pb deposit where skarn mineralization was distinguished, higher Cu, Pb and As concentration was determined. Eleven boreholes have been run into the deposit with the total length of 1500m. The 650,000t reserve @3.63% ΣZn+Pb, 170,000t of which @1.76ppm Au was determined (Kavoshgaran Consulting Engineers, 2010).

The mineralization in Nodoushan Zn-Pb deposit which obviously followed structural controlling factors consisted of both sulfide and later stage minerals. The mineralization consists of earlier sulfide minerals as disseminated pyrite followed by ore minerals concentrated along faults and fractures (hydrothermal conduits) such as sphalerite, galena, pyrite and chalcopyrite. Some acicular hematite and negligible magnetite as well as barite veinlets were also distinguished.

Sphalerite is the most abundant ore at the deposit. Anhedral minerals sometimes demonstrate embayment which indicates later stage corrosion and earlier formation. Sphalerite is mainly concentrated along veins, demonstrates considerable chalcopyrite exsolution (disease) especially at the margins or when the sphalerite is cut across by later stage veinlets such as galena or chalcopyrite on one hand and contain high iron on the other hand. This observation which trivially suggests sphalerite formation prior to later stage chalcopyrite and

galena, suggests thermal shock (Ramdohr, 1969; Barton and Bethke, 1987). Further studies on sphalerites demonstrated that they fell into two categories: 1) high-Fe sphalerites (generally more than 2% Fe) with chalcopyrite disease 2) low-Fe sphalerites (generally less than 2% Fe) lacking or having negligible chalcopyrite disease which can be observed in Fig.4 and 4d.

Galena which is developed at the same time or later than sphalerite as veinlets (Fig. 4- b and c) is characterized by triangular pits; the curve in their linear features indicates deformation resulted from tectonic activities and fault displacement involved in their development (Fig. 6- d). Galena is more or less associated with chalcopyrite that suggests hydrothermal fluids rich in lead had considerable copper content to develop such minerals, but the Zn content had depleted earlier along with part of their iron content.

Chalcopyrite as a late stage sulfide mineralization occurred as anhedral grains in smaller quantity than sphalerite and galena. Lack of characteristic features and its ductile nature do not provide us with clues for continuous stress along controlling fault on ore concentration. However, it demonstrated the halo as far as which copper disseminated through the mineralizing system as well as serves as a clue for tracking thermal shock in high-Fe sphalerites (Fig.4- a).

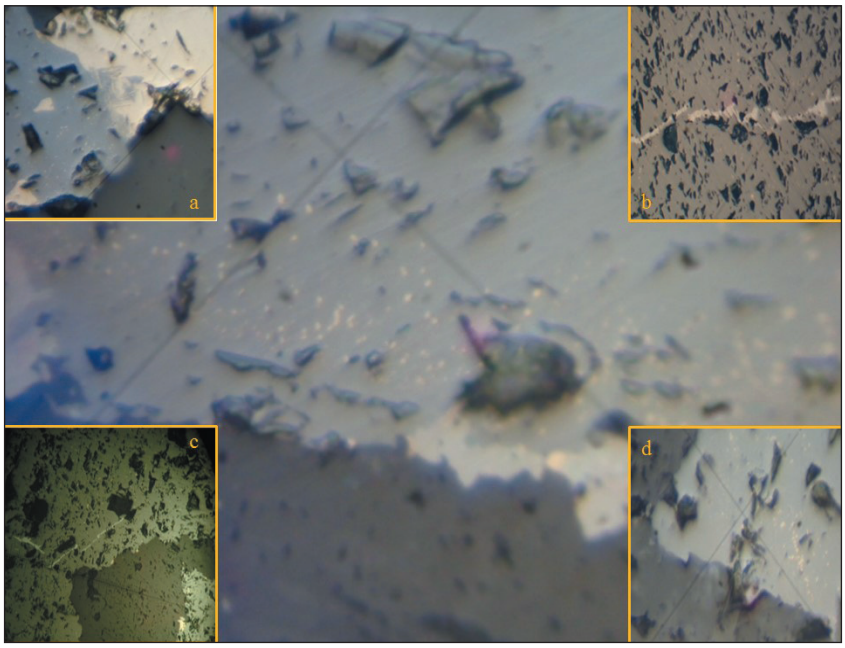

Fig. 4- Major figure chalcopyrite exsolved at the sphalerite margins. a) later stage chalcopyrite solving sphalerite; b) galena veins cut across the sphalerite with chalcopyrite exsolution around the vein; c) another galena vein cutting across the sphalerite; d) chalcopyrite exsolution at the sphalerite margin.

Pyrite which is the most abundant mineral is observed as disseminated euhedral cubes in volcanic rocks as the first generation pyrite (Fig. 2- d and 5- b). Later stage pyrite developed along faults and is associated with other sulfide minerals. Its brittle nature serves as a good sensor to deformation and demonstrates the presence of such stresses as crushing and brecciation (Fig. 6- b and c) that can be observed in polished sections.

The base metal mineralization was mainly as open space fillings veins and veinlets as well as minor breccia, but, some fossils were replaced by ore minerals, served as geochemical traps (Fig. 5- f and k and 8- e). Cu, Pb and As concentration was detected just in one skarn sample.

The aforementioned sulfides could be observed mainly in samples deeper than 40 m (according to polished section studies on 234 samples from 11 boreholes up to the depth of 200m) as later stage supergene conditions led to the conversion of sulfide minerals into secondary minerals such as carbonates, sulfates and oxides. Old mining activities at Nodoushan which was as a 4-m long cave, was lined by secondary lead and zinc minerals on its ceiling and walls such as cerussite, hemimorphite and hydrozincite crusts, sometimes with colloform texture. Other oxide minerals were malachite, azurite, Fe-oxides (Fig. 5- j) and hydroxides, dendritic manganese oxides and considerable amounts of gypsum fibers in old trenches. Further studies on the

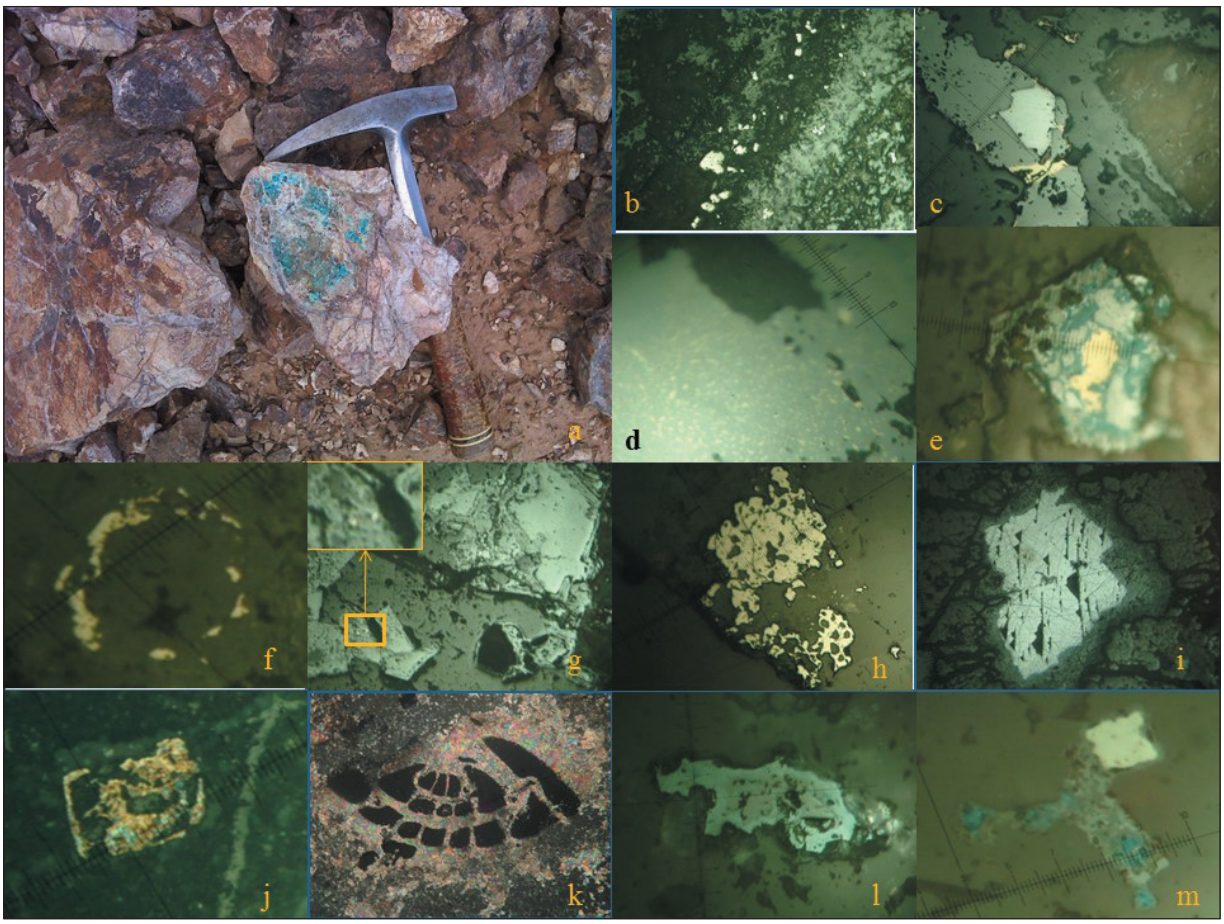

Fig. 5- a) Silicified and mineralized rhyo-dacitic tuff which is oxidized to malachite; b) small pyrite grains along the veins; c) sphalerite vein intruded by later stage galena and chalcopyrite; d) extensive chalcopyrite inclusions in sphalerite (34.5m); e) chalcopyrite oxidation to chalcocite and covellite (38.5m); f) Atoll-like pyrite indicates earlier structure probably fossil replacement (33m); g) complete replacement of pyrite by goethite with enlarged picture at the top left with two small remained yellow pyrite; h) engulfment in pyrite; i) galena oxidizing to cerussite and anglesite; j) oxidized pyrite crystal (13.5m); k) Ore replacement in fossil (79 m); l) Chalcocite conversion to digenite; m) pyrite oxidation to covellite (23m).

polished section demonstrated more mineralogical variation during supergene processes as chalcocite, bornite, digenite, covellite (Fig.5- e, l and m), anglesite (Fig.5i).

Fluid inclusion studies on sphalerite and quartz demonstrated 172-254˚C homogenization temperature and 5.01-13.07 wt% NaCl equivalent which suggested hydrothermal vein-type mineralization at Nodoushan (Sepehrifar, 2011). The samples studied were from two core drills. The northern core drill (with weak skarn signatures) with the less depth (28m) demonstrated a bit higher fluid inclusion temperature and salinity compared to the sample from the middle core drill (main epithermal vein type) with the higher depth (44m).

5- Structural controls

The area is tectonically active as evidenced by DehShir-Baft major fault near to the study area, the density of faults, development of dikes, dissected and displaced veins as well as its situation at the western margin of CIM and proximity to Sanandaj-Sirjan metamorphic volcanic belt. This indicates the role of structural controlling factors in channelizing hydrothermal fluids emanated from or heated by heat sources. These features can be observed at the small scale on satellite images (trans-tensional faults) up to microscopic scale (subgraining, brittle deformation and undulous extinction in quartz, plagioclase and pyrite).

The complex tectonic activities in the area played a major role in the localization of fault-controlled hydrothermal system with field evidences grading into microscopic scale. The development of veins and veinlets accompanied by silica, was later associated with late stage carbonates. The ore minerals associated with quartz and feldspar veins and veinlets demonstrate fringes which indicate tension and dilatant veins. The tectonic activity which involved in the channelizing hydrothermal fluids and its emplacement in

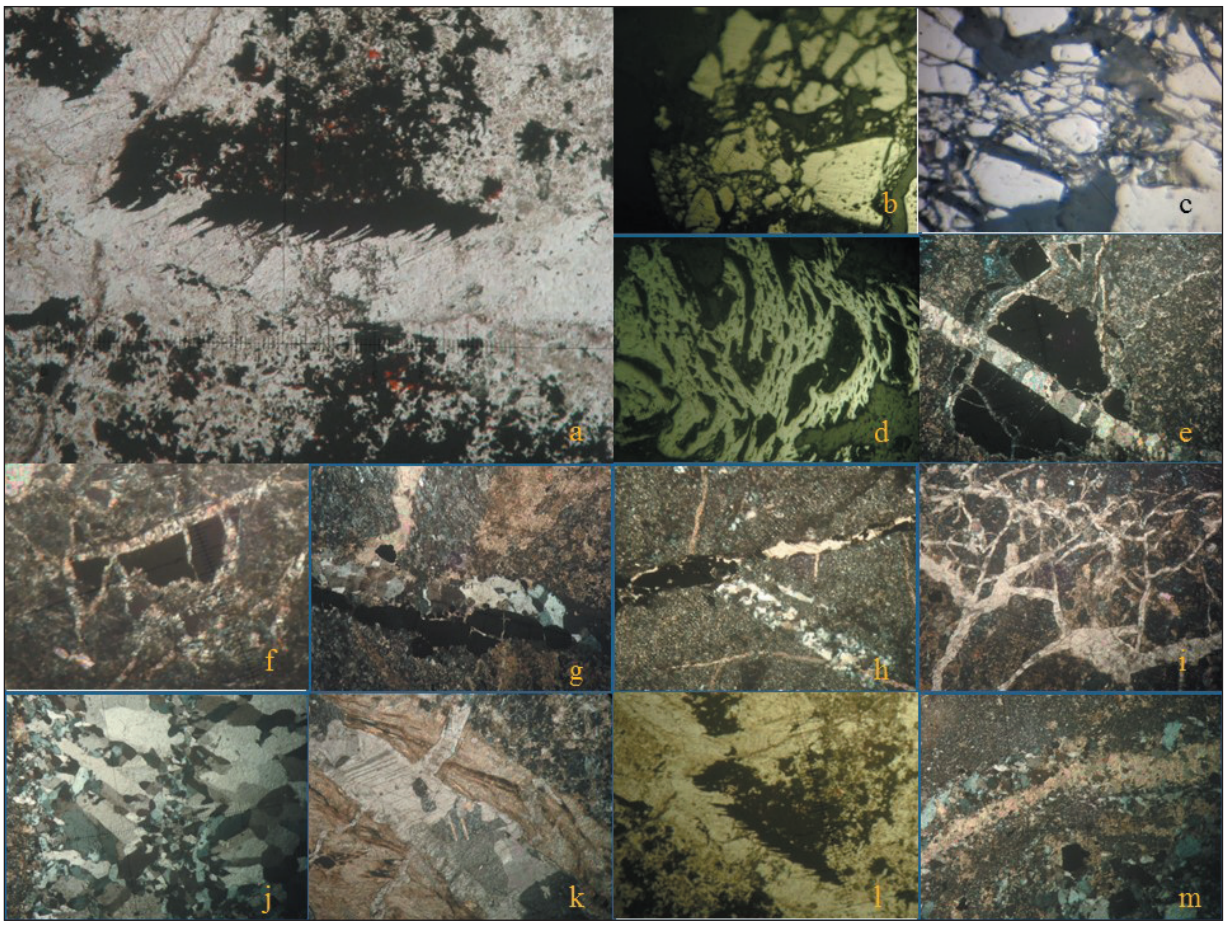

Fig. 6- a) syn-tensionional vein associated with ore (71m); b) pyrite brecciated along vein; c) pyrite brecciated along vein (34.5m); d) tectonic activities which led into deformation in galena triangular pitch-falls (45m); e and f) later stage carbonate veins cut across earlier ores and encompassing them (71m); g) mineralization as opaque minerals associated with quartz vein; h) late stage ore associated with carbonate vein which cuts across earlier quartz vein (37.5m); i) dense stockwork-like carbonate veins; j) subgraining in quartz veins; k) late stage carbonate veins contaminated with iron oxide in earlier stage (vein margin) and barren at the late stage (vein center); l) late stage veins cutting across earlier ore (71m); m) late stage calcite vein which filled the center of the earlier quartz vein (18.5m).

the fractures, later caused ore oxidation and grade reduction (Fig. 6- e and f) as these fractures was the most susceptible areas to continuous tectonic activities to displace along them and serve as the channels to conduct surface water to the sulfide minerals.

6- Alteration

Alteration which localized along the Nodoushan fault could be obviously observed at the outcrop as argillic white patch of clay minerals, especially to the northern parts of the deposit (Fig. 7). The other alterations observed in the study area are silicification and dolomitization. The strongest silicification was observed along the fault which may suggest hydrothermal fluid emanating from the granite, served as a brittle preparation for mineralization. Furthermore, propylitic alteration was widespread through the area, especially near the fault. The main argillic alteration outcrop was more than 20m wide and 40 m long that stretched along (Permian?) limestone and Eocene volcanic thrust contact. This trend followed NW-SE fault passing through the deposit which served as a conduit for the hydrothermal fluids which led into alteration and ore deposition. The white outcrop was likely advanced argillic alteration zone, where the trench No.7 was run.

The XRD results from the surface samples demonstrated illite, montemorillonite, jarosite, chlorite, epidote and silica which confirmed argillic and propylitic alteration. Kaolinite was also detected from the samples taken from the depths (based on the data from Kavoshgaran Consulting Engineers, 2010).

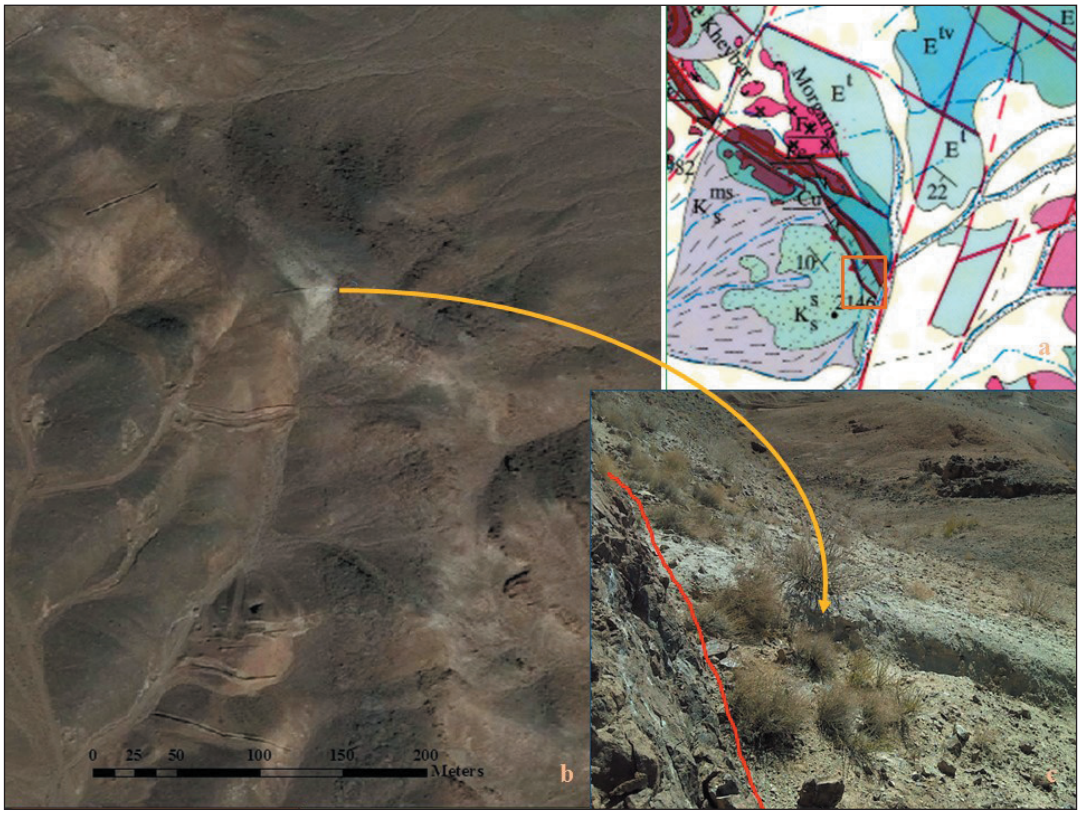

Fig. 7- a) part of 1:100000 geological map of Kafe Taqestan in the study area (Qalamqash and Mohammadiha, 2005); b) white alteration patch on SAS image along with other trenches; c) Field view (looking south) which demonstrates alteration at the contact of Permian carbonates and Eocene volcanic rocks and tuffs.

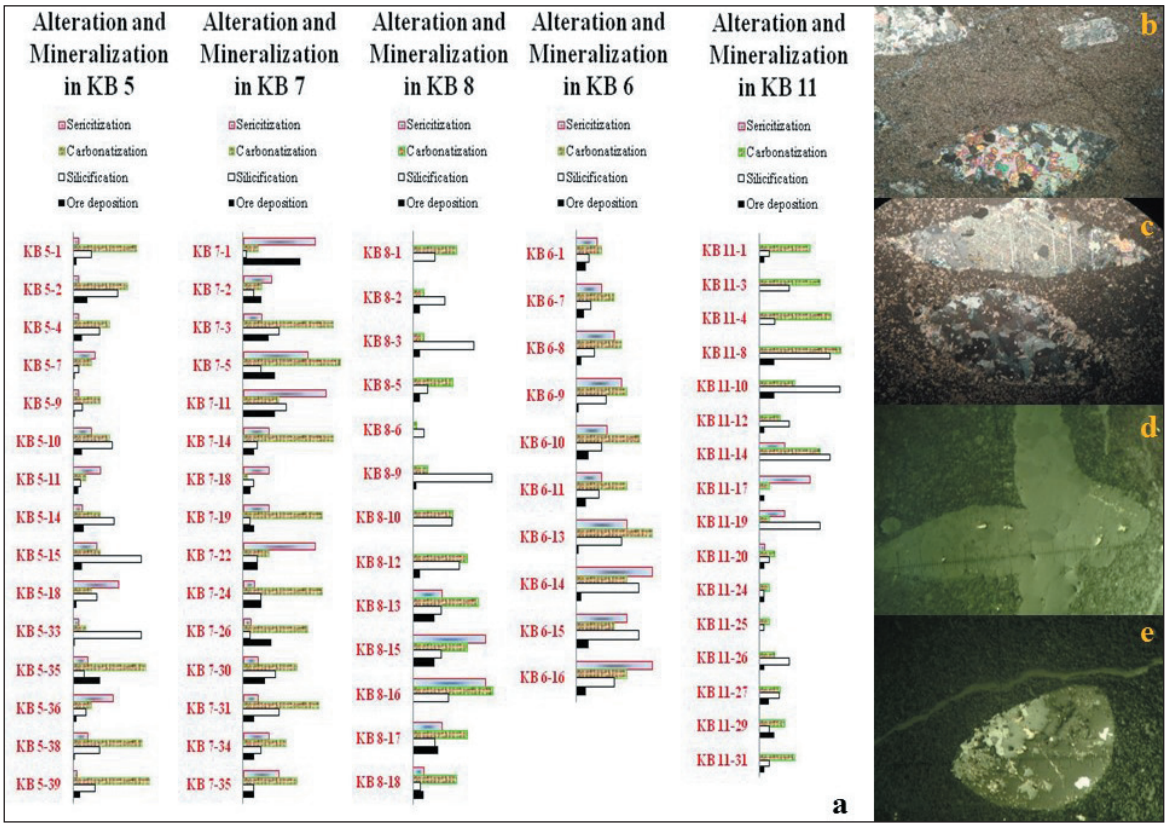

Fig. 8- a) Relative alteration extent and ore minerals in thin sections within 5 logs in Nodoushan Zn-Pb deposit from KB5 in the South to the KB11 in the North; b, c, d and e) microscopic thin sections illustrating epidote (b) and silica and calcite (c) pyrite (d) and sphalerite, galena and pyrite (e) replacement in fossils.

Signatures of alteration in microscopic thin and polished sections as selective replacements in fossil also helped us to detect changes in geochemical fluids channeling the deposit due to their higher susceptibility to these fluids with respect to the surrounding minerals which served as biochemical traps (Fig. 8- b, c, d and e and 9). The surface strong but small alteration at the northern part of the deposit as well as fossil replacements evidenced by quartz, calcite, epidote, iron oxides as well as partial or complete ore replacement at different depths indicate alteration associated with mineralization (Fig. 3). The comparison of ore minerals abundance with the relative three alteration types distinguished in five logs demonstrated good harmony with silicification. A correspondence was also observed between carbonatization and ore minerals in log KB8 (Fig. 8- a). Numerous late stage calcite and dolomite veins and veinlets from samples of KB5 at the depth of 80m, cutting across earlier stage quartz veins was the last stage of alteration.

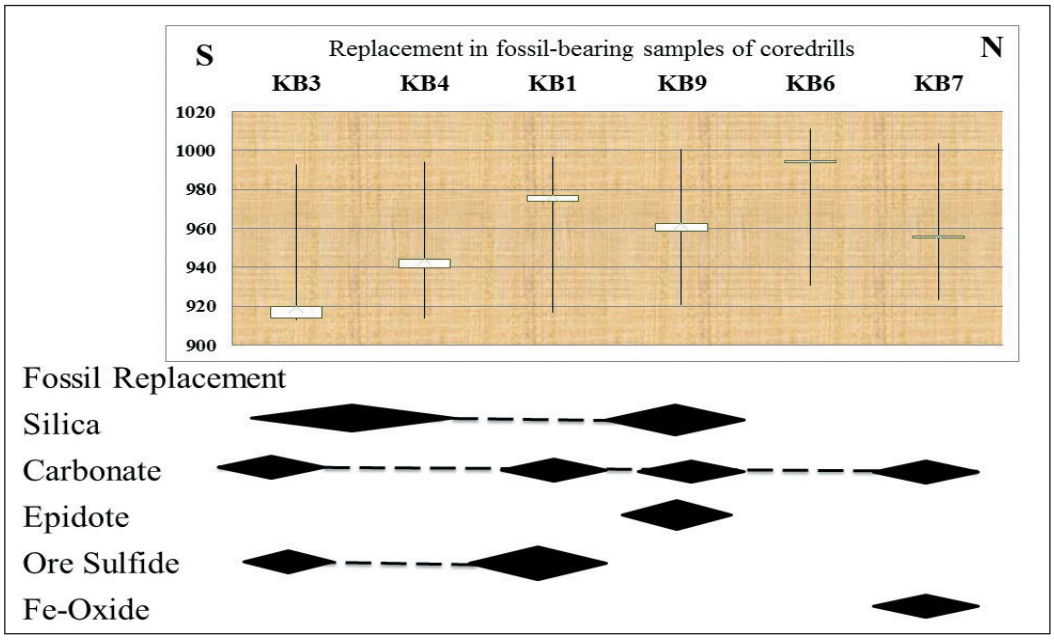

Fig. 9- fossil replacement with alteration minerals.

Geochemical studies on the samples which obvious metasomatism was distinguished in 10 thin sections (out of the 144) demonstrated negligible enrichment and depletion in their chemical composition, mostly in Fe and Mg, followed by Mn, S, Na. Just two samples had associated chemical enrichment and one sample with distinct Pb, Cu and As contents. Generally speaking, metasomatism did not involve significant enrichment and alteration.

7- Geochemistry

The comparison of samples deeper than 20m to samples shallower than 20m demonstrates that Zn, Pb, Cu, Cd, As, Ag, Au, W and S were concentrated in deeper samples. The content distribution of elements through the samples of all logs demonstrates that zinc (max. 11.5%) is the dominant commodity of the deposit followed by lead (max. 13.4%), where the lead increases over zinc is in few samples. The major concentration of commodities was mainly at the depth of 78 to 93 which was the case for copper, arsenic, cadmium, tungsten and silver with maximum values of 13134, 2159, 2223 ,2331, 263ppm respectively. 5 out of 9 samples with gold content more than 3ppm fall in this depth range with maximum 12 ppm. The overall geochemical analysis indicates that the main mineralization zone was located at depth in a 15m depth range, where deeper the concentrations decreased abruptly. There were four other minor horizons at lower depths of 30, 40, 60 and 70 m. The dominant Zn along with Pb and Cu demonstrates that the ore has been transported through chlorine complexes.

The geochemical correlation of elements in the top mineralized core drill No.5 indicates that there is a very good correlation (more than 0.9) among four sets of elements which are as following: 1) zinc with cadmium, copper and tungsten, 2) arsenic and copper 3) lead and silver 4) phosphorus with titanium, vanadium and scandium. Good correlations (0.8) among elements are as following: 1) arsenic with zinc, cadmium and tungsten 2) gold with cadmium and tungsten 3) copper with lead and silver 4) silver and cadmium.

The aforementioned correlations as well as factor analysis of the chemical results of samples suggests that zinc and lead which were the dominant commodities of the deposit, had a close association with Cu, Cd, W, Au, Ag, As which may be of first or second class, however the high rate of correlation justifies their match with epithermal vein type deposits.

The comparison of samples deeper and shallower than 20m demonstrated that Na, K, Al were concentrated in shallow samples while Ca and Mg were concentrated at depth, with Fe, Mn and Ti of the same concentration at the shallow and deep samples (Fig. 10). The higher concentration of Ca and Mg indicated carbonate alteration including calcite alteration and dolomitization, while the process involved in mineralization did not contributed to the Fe, Mn and Ti concentration either as the different source for commodities or different complexing agents involved in their transportation. However, one should be careful on the presence of adjacent dolomite and dolomitic limestone that may play an important role in contributing to the hydrothermal fluids when the plutons intruded the volcanic and sedimentary rocks as the source magma may not provided the hydrothermal fluids with its own carbonate complexes.

Comparison of silver and gold in the core drills indicated that the Ag:Au ratio is never less than 5 with the maximum 2700 and average of 193. This ratio tends to decrease northward where strong argillic alteration was observed that is reflected in less than 0.8 correlation between gold and silver (0.66). The average Ag/Au ratio more than 50 maybe considered as a parameter ranging from IS to HS epithermal deposits (Volkov et al., 2013).

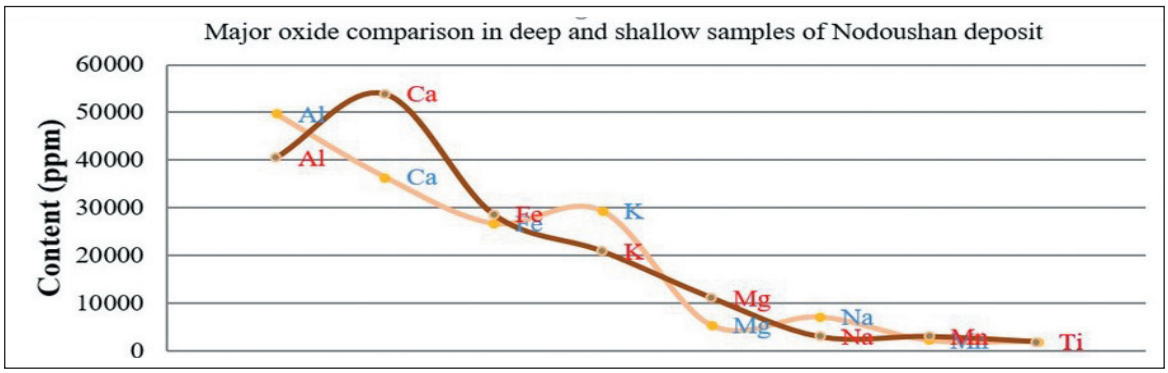

Fig. 10- The higher Ca and Mg content in the brown deep samples (more than 20m deep) compared to shallow samples may indicate carbonate alteration.

The analysis result of more than 230 samples demonstrated that the mineralization favours zinc with some tendency towards lead. Higher copper association with zinc rather than lead may amounts to maximum equal copper and zinc in lower lead content samples. It suggests more chemical affinity of copper with zinc rather than lead (Fig. 11).

The geochemical characteristics of intrusive bodies suggest a volcanic arc setting which is illustrated in Fig.12. This tectonic setting is favorable for epithermal vein-type mineralization whether HS, LS or IS. A comprehensive study on such type of mineralization demonstrated that such mineral deposits are in close relationship with magmatic arc settings. The plutonic bodies studied earlier by Yajam (2005) and the six samples in the study area confirms such setting for the intrusive bodies.

8- Geological and mineralization history

Nodoushan mineralization history is closely involved in its geological history. The following stages can be suggested for part of its history:

1) Acid to intermediate volcanic, volcano-sedimentary and tuff deposition sometimes associated with disseminated pyrite, hematite and barite and Eocene fossil-bearing limestone.

2) Tectonic processes involvement in faults and displacements (including Permian? carbonates) which ran for a long period with changing characteristics.

3) Intrusion of water-bearing diorites (myrmekitic textures) and development of iron skarn deposits to the north and at the northern part of the deposit.

4) Intrusion of granite body which involved in both Zn-Pb as well as dolomite and calcite veins dissolved from adjacent Permian? dolomite and dolomitic limestone.

5) Continuation of stress during the mineralization which extends afterwards is evidenced by graining and undulous extinction in quartz. Hydrothermal alteration following faults, curved linear features in galena, grasslike ores tending middle of the veins and carbonate veins cut across quartz veins all indicate that the area is tectonically active.

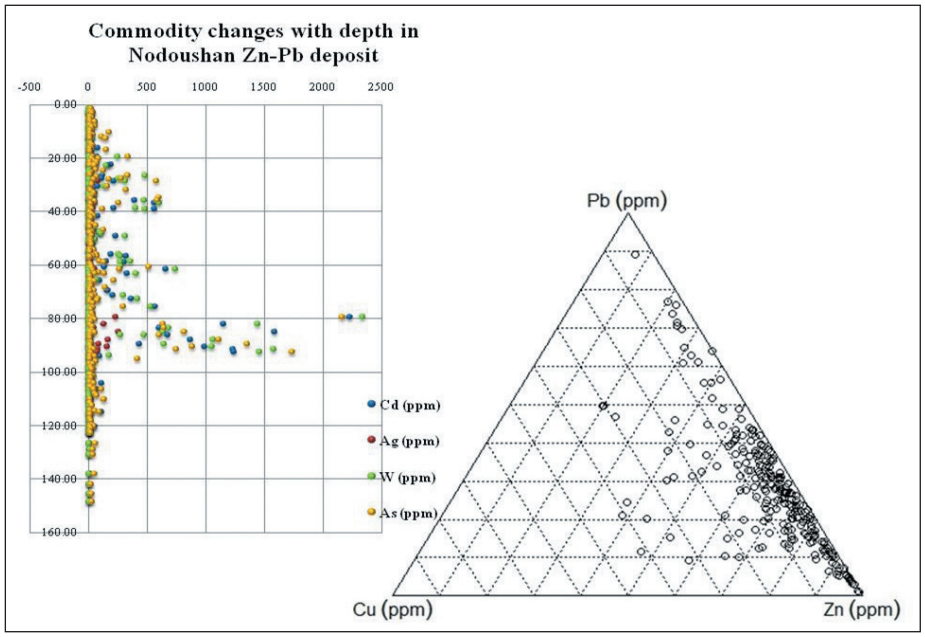

Fig. 11- Ternary diagram illustrating Zn-Pb-Cu relative content which indicates that the deposit is Zn-dominated (right), The content changes in Cd,Ag,W and As with depth. The mean content from most to least are as folllowing: W, Cd, As, Ag, the maximum of which nest in ore horizon at the depth of 78 to 92m (left) .

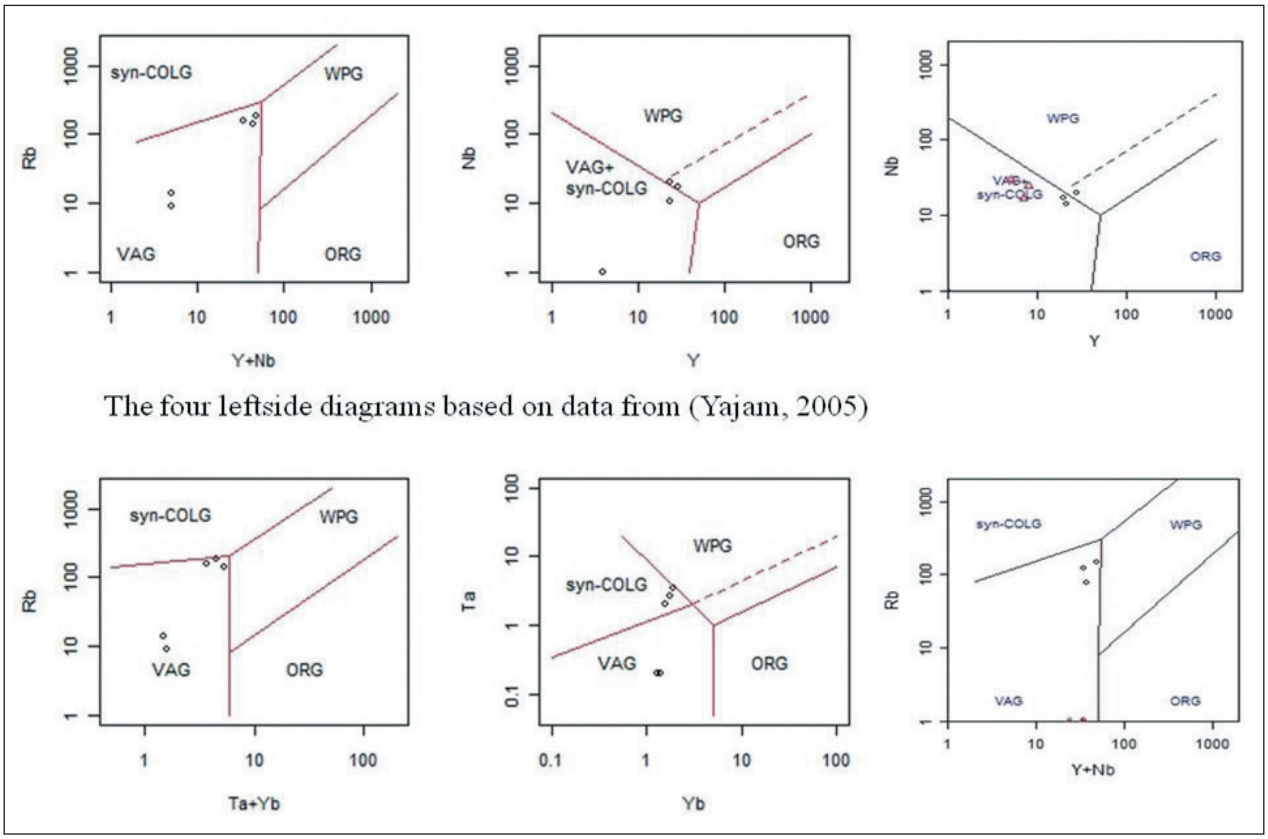

Fig. 12- Tectonic discrimination diagram (Pearce et al., 1984). The two righthandside diagrams are granite samples in black and dike samples in red.

The late stage carbonate veins may indicate secondary boiling at the deposit.

6) Oxidation of early sulfides along faults and at the surface, esp. on the ceiling and walls of the old cave.

9- Conclusion

Extensive silica veins and veinlets associated with sulfide minerals indicate epithermal vein system which is Zn-dominated based on geochemistry, but the considerable role of structural controlling factors is highlighted far more. The paragenetic sequences of ores which indicate earlier sphalerite deposition is confirmed by later chalcopyrite disease as a result of thermal shock of following Pb- and Cu-bearing hydrothermal fluids. The deposit which is preceded by iron skarn mineralization, inherited part of its iron content as high-Fe sphalerites and late stage iron-contaminated carbonate veins. The most important mineralization is epithermal. Skarn and (fossil) replacement are of less importance. The situation of the deposit at the transitional zone between Cu-realm of Dehaj-Sarduyieh to its northern Pb-Zn deposits with second class iron deposits attaches higher importance to the genesis of such types of deposits.

References

Ahmad, T. P., 1993- Geochemisty and Petrogenesis of Urumiah-DokhtarVolcanics Around Nain and Rafsanjan Areas: A Preliminary Study, Treatise on the Geology of Iran. Iranian Ministry of Mines and Metals.

Barati, B., 2017- Detailed exploration and mineral-geological mapping in Nodoushan Iron area (yazd Province) on the scale of 1:1000. Geological Survey of Iran.

Barton, P. and Bethke, P. M., 1987- Chalcopyrite disease in sphalerite: Pathology and epidemiology. American Mineralogist , 451-467.

Bazin, D. and Hübner, H., 1969- Copper deposits in Iran, Report No.13. Geological Survey of Iran.

Bazin, D. and Hubner, H., 1968- Khut copper prospect. Geological Survey of Iran.

Berberian, M. and Berberian, F., 1981- Tectono-plutonic episodes in Iran.

Berberian, M. and King, G. C. P., 1981- Towards a Paleogeography and tectonic evolution of Iran. Canadian Journal of Earth Science, 18, 210-265.

Brown, T. J., Idoine, N. E., Raycraft, E. R., Shaw, R. A., Deady, E. A., Hobbs, S. F. and Bide, T., 2017- World mineral Production 2011-2015. British Geological Survey.

Etemadi, B., Taghipour, B., Qobadi, A., Eslami, A. and Salimidarani, M., 2012- Petrography and tectonic setting of Tertiary igneous rocks in Nodoushan, SW Sadough, Yazd Province. Journal of petrology , pp. 13-26.

Giese, P. M., 1984- The Crustal Structure in Southern Iran Derived from Seismic Explosion Data. Neues Jahrbuch Geologie und Palaeontologie Abhandlung , 168, 230-243.

Hakemi, A., 1997- Shahdad - Archaeological excavations of a Bronze Age center in Iran. Reports and Memoirs 27. Rome.

Hauptmann, A. R. S., 2003- Early Bronze age copper metallurgy man and mining-Mensch und Bergbau. Deutsches Bergbau Museum Bochum.

Kavoshgaran Consulting Engineers, 2010- Final report on Exploraton at Nodushan polymetallic deposits, Yazd province. Geological Survey of Iran.

Lotfi, M., Mirmohammadsedghi, M. M. and Omrani, J., 1993- Mineral distribution map of Iran. Geological Survey of Iran.

Makizadeh, M., Rahgoshay, M., Daliran, F., 2007- Development of andraditic garnets in Surk iron deposit. Research Journal of Isfahan University, pp. 157-168.

Minook Consulting Engineers, 1993- Preliminary exploration and Geological mining mapping of Surk Iron ore -Nodoushan, Yazd on the scale of 1:5000.

Momenzadeh, M., 2005- A glimpse on ancient mines and mining in Iran. Journal of Cheshmeh, No.5 (in Persian). , pp. 7-11.

Najafi, A., Motevali, K. and Abdi, M., 2012- Mineral distribution map of Iran. National Geosciences Database of Iran, Geological Survey of Iran.

Omrani, J., Agard, P., Whitechurch, H., Benoit, M., Prouteau, G. and Jolivet, L., 2008- Arc-magmatism and subduction history beneath the Zagros Mountains, Iran: A new report of adakites and geodynamic consequences. Lithos , 380 –398.

Qalamqash, J. and Mohammadiha, K., 2005- Geological map of Kafe Taqestan on the scale of 1:100000. Map . Geological Survey of Iran.

Ramdohr, P., 1969- The ore minerals and their intergrowths. Pergamon Press.

Schreiner, M., 2002- Mineralogical and geochemical investigations into prehistoric smelting slags from Tepe Sialk/Central Iran. Institute für Mineralogie, TU Bergakademie Freiberg.

Sepehrifar, P., 2011- Ore Genesis of Nodoushan Polymetallic deposit (In Persian). Dissertation . Research Institute for Earth Sciences, Geological Survey of Iran.

Shahabpour, J., 2007- Island-arc affinity of the Central Iranian Volcanic Belt. Journal of Asian earth sciences , 652-665.

Shahsavari Alavijeh, B., Rashidnezhad-Omran, N. and Corfu, F., 2017- Zircon U-Pb ages and emplacement history of the Nodoushan plutonic complex in the central Urumieh-Dokhtar magmatic belt, Central Iran: Product of Neotethyan subduction during the Paleogene. Journal of Asian Earth Sciences , 283–295.

Taghipour, B. and Makizadeh, M. A., 2011- Skarn petrogenesis related to Aliabad-Darrehzereshk porphyry copper intrusive body, Yazd. Journal of Economic Geology, 1 (3), 79-92.

Taghizadeh Khajooee, N. and Sheykhi Karizaki, H., 1998- Preliminary exploration studies for metallic complexes in Nodoushan district, Yazd. Danesh Zamin Consulting Engineers.

Volkov, A. V., Chizhova, I. A., Yu, V., Alekseev, A. and Sidorov, A., 2013- Variations of the Ag/Au Index in Epithermal Deposits. Doklady Earth Sciences, 911-914.

Yajam, S., 2005- The study of geochemistry and petrology of plutonic rocks of SW Nodoushan. M.Sc. Tehran, Tehran, Iran: Tarbiat Moallem University.

Yazdi, M., 1992- Economic geology and petrology of Khut deposit, Yazd. Shahid Beheshti University, Tehran, Iran (M.Sc. Thesis).